



Surface sorption and surface diffusion of NpO_2^+ with poorly crystallized ferric oxide

Shinya Nagasaki*, Satoru Tanaka, Masaru Todoriki, Atsuyuki Suzuki

Department of Quantum Engineering and Systems Science, The School of Engineering, The University of Tokyo, 7-3-1 Hongo, Bunkyo-ku, Tokyo 113, Japan

Abstract

The sorption of NpO_2^+ onto synthetic poorly crystallized ferric oxide was studied by conducting batch experiments in the pH range from 4 to 8 as well as adsorption isotherm studies and constant boundary condition studies. The sorption process was characterized by two steps. The first step was a rapid reaction between the bulk solution and the external surfaces of the poorly crystallized ferric oxide. In this step, NpO_2^+ was sorbed on the external sites of the poorly crystallized ferric oxide by formation of an inner-sphere complex. The second step was a slow and rate-limiting reaction wherein the NpO_2^+ diffused through small pores in the poorly crystallized ferric oxide. By taking account of these two steps and the mass balance of NpO_2^+ in the poorly crystallized ferric oxide, we applied the diffusion model to our experimental results, and evaluated the surface diffusion coefficient of NpO_2^+ at $2.0 \times 10^{-13} \text{ cm}^2 \text{ s}^{-1}$. © 1998 Elsevier Science S.A.

Keywords: NpO_2^+ ; Poorly crystallized ferric oxide; Sorption; Surface diffusion

1. Introduction

Neptunium-237 is considered to be a possible long-term hazard in ecosystems [1], because of its long half-life ($T_{1/2} = 2.14 \times 10^6$ years) and its mobile nature under aerobic conditions due to the high chemical stability of the pentavalent state, NpO_2^+ . An understanding of Np sorption behaviour is required to describe the transportation of it in surface and groundwater systems quantitatively [2].

Under aerobic conditions, the weathering of iron-containing primary rocks leads to the formation of secondary iron oxide minerals. Precipitates of these minerals can be found in surface and groundwater systems. These minerals show a varying degree of crystallinity and can occur as colloids or coatings. These iron oxides, especially Fe-hydroxides, e.g., ferrihydrite, are much better scavengers of trace elements in natural waters [3]. Therefore, the sorption data of Np on iron oxides will be required to describe the mobility of Np in natural waters. Some studies

on sorption of Np onto iron oxides have been performed and sorption models are based on the assumption that there is a rapid equilibrium established between Np and iron oxides [4]. Equilibrium models, however, have generally not been successful at simulating trace element distribution [5,6]. This lack of success results from the failure to consider kinetic aspects of trace element sorption [7,8]. Studies on the sorption of inorganic elements, such as arsenate, nickel, cadmium, strontium and zinc, on metal oxides suggest that a two-step reaction is involved [9–13]. The first step is a rapid, reversible reaction between bulk solution phase and sorbent external sites. The second step is a slow process wherein the inorganics sorbed on the surface slowly diffuse into the micropores of the oxides. Recently, Axe and Anderson have experimentally studied the sorption of Cd and Sr in ferric oxides and successfully predicted the sorption kinetics by considering the two-step processes [9,10]. For Np, no such a process has been reported in the literature. Therefore, it is necessary to investigate sorption, diffusion and reaction within the iron oxides.

In the present work, the sorption of NpO_2^+ on ferric oxide was investigated in the pH range from 4 to 8 by batch experiments, to examine whether NpO_2^+ is sorbed on

*Corresponding author. Tel.: +81 3 3812 2111 (ext.) 6995; fax: +81 3 58006856; e-mail: nagasaki@q.t.u-tokyo.ac.jp

ferric oxide by a two-step reaction or not, according to the experimental and analytical procedure of Axe and Anderson [9,10].

2. Experimental

2.1. Chemicals

All experiments were performed in a glove box (<1 ppm O₂) filled with highly pure nitrogen (purity=99.999%) at 25°C. All chemicals except ²³⁷Np solution were reagent grade and used without further purification (Wako Pure Chemical Industries Co. Ltd., Japan). Water was prepared from doubly distilled water by further purification with Milli-Q system (Millipore) and ultrafiltered by use of a 2 nm pore size ultrafilter (UFPI, Millipore) immediately before use. Neptunium-237 in 1 M HNO₃ was purchased from LMRI, France. By liquid-liquid extraction of the Np solution with *n*-octyl(phenyl)-*N,N*-diisobutylcarbamoylmethylphosphine oxide, a Np(V) stock solution was prepared [14]. The concentration of Np(V) stock solution was 1×10⁻⁵ M. The oxidation state and speciation of Np were spectroscopically confirmed to be pentavalent and NpO₂⁺.

The ferric oxide was prepared and aged using the procedure described by Matijevic and Scheiner (FeCl₃-HCl system) [15]. The crystallinity of the ferric oxide was analyzed by XRD and it was found that the solid sample prepared in the present work was the poorly crystallized ferric oxide (PCFO). The amount of H₂O included in this solid sample was measured by TG/DTA (Shimadzu TGA-600) and found to be 17.1 weight percent per one-gram of the solid sample. The surface area and the pore size distribution of freeze-dried PCFO were measured with BET method (Shimadzu ASAP-2010) and a mercury porosimeter (Shimadzu Poresizer-9320), respectively. The specific surface area was evaluated at 35.5 m² g⁻¹. The porosity was 0.5 and the pore size distribution was shown in Fig. 1. The vertical axis (left side) of Fig. 1 represents the ratio of pore volume to the corresponding pore diameter per one-gram of the solid sample. Almost all pore diameters were less than 10 nm. The particle size distribution in the aqueous phase was measured with a particle counter (Shimadzu SALD-2000) (Fig. 1). In SALD-200, the particle size distribution is estimated by Fraunhofer theory, Mie theory and Side Scatter theory, but there is a possibility that larger particles mask the presence of smaller particles. We will check the particle size distribution with another method such as microscopic technique (TEM/SEM) in the near future. According to Matijevic and Scheiner, the shape of PCFO used was assumed to be spherical.

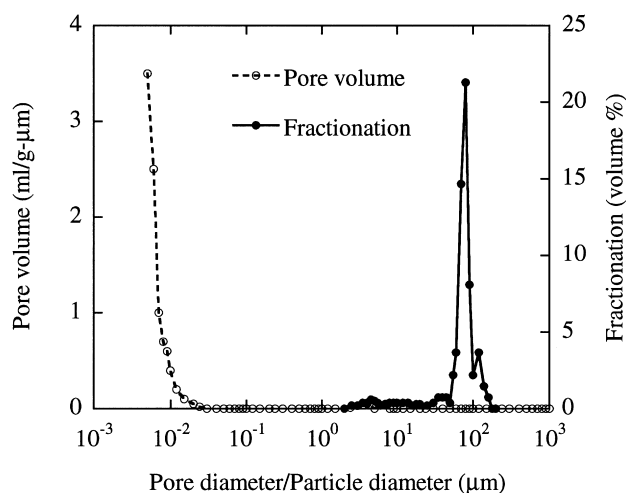


Fig. 1. Pore size distribution and particle size distribution of poorly crystallized ferric oxide.

2.2. Sorption of NpO₂⁺

2.2.1. pH dependence

In this section, the dependence of the sorption of NpO₂⁺ onto the external sites of PCFO on pH was investigated. PCFO suspension was poured into a polypropylene tube and a spike of Np(V) stock solution was added. The pH was adjusted from pH=4 to pH=8 by using CO₂-free NaOH. The ionic strength was adjusted by addition of 1×10⁻² M NaClO₄. The concentrations of Np and Fe were 1×10⁻⁸ and 1×10⁻² M, respectively. The tube was closed tightly, shaken gently for 4 h and then centrifuged. A sample was taken from the supernatant of the tube and ultrafiltered with UFPI. The activities of ²³⁷Np (29.3 keV) in the sample and in the ultrafiltrate were measured with a well-type Ge detector. The sorption of Np onto the tube wall was negligibly small. To make sure that no sorption of Np occurred during the ultrafiltration process the sorption sites of the ultrafiltration membranes were blocked by preconditioning of these materials. The filters were preconditioned by following a procedure described by Nitsche [16]. Hence, the influence of preservatives in the ultrafilter could be considered to be neglected and the influence of sorption onto the ultrafilter was avoided. Batch experiments were conducted in triplicate. One series of batch experiments were carried out in 1 M NaClO₄ in order to determine the influence of ionic strength on the sorption.

2.2.2. Adsorption isotherm

Isotherm of NpO₂⁺ sorption onto the external sites of PCFO was measured by batch technique. The PCFO suspension was poured into a polypropylene tube and a spike of Np(V) stock solution was added. The pH was adjusted to pH=6 by using CO₂-free NaOH. The ionic strength was adjusted to 1×10⁻² M by using NaClO₄. The

concentrations of Np initially added were ranged from 1×10^{-9} M to 1×10^{-7} M. These are below the solubility of $\text{NpO}_2\text{OH(s)}$ [17]. The concentration of Fe was 1×10^{-2} M. Forty-two tubes were closed tightly and shaken gently for a pre-decided period (1, 2, 4, 24, 48 and 96 h). After each pre-decided period, seven tubes, of which the initial Np concentrations were different each other, were centrifuged. The subsequent experimental procedure was same as that mentioned above.

2.2.3. Sorption in micropore

To measure the sorption of NpO_2^+ in a micropore of PCFO, a constant boundary condition technique proposed by Axe and Anderson [9] was performed in duplicate. In this experiment, Np concentration in the bulk aqueous phase was kept approximately constant by measuring Np concentration in the aqueous phase continually and by adding the Np(V) stock solution as needed. The initial concentrations of Np, Fe and NaClO_4 were 1×10^{-8} M, 1×10^{-2} M and 1×10^{-2} M, respectively. The pH was adjusted to pH=6. Fifteen tubes were vigorously shaken for a pre-decided period (1, 12, 48, 96, 120, 240, 360, 480, 600, 840, 1080, 1320, 1560, 1800 and 1920 h). After each pre-decided period, a tube was centrifuged. The subsequent experimental procedure was same as that mentioned in Section 2.2.1.

3. Results and discussion

3.1. pH dependence and isotherm of NpO_2^+

The sorbed amount of Np is shown as a function of pH in Fig. 2. The steep S shaped curve characteristic indicates

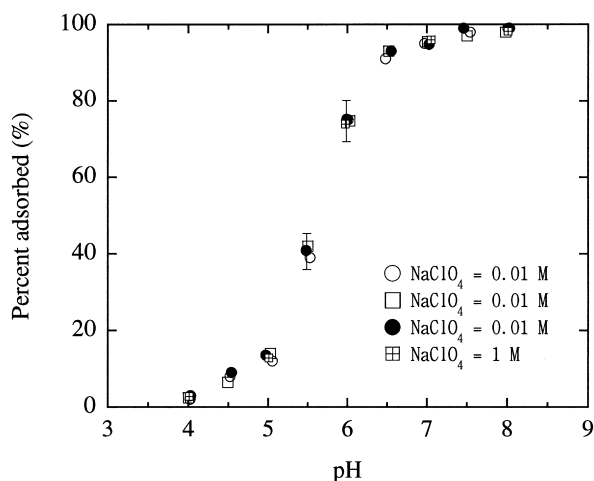


Fig. 2. pH dependence of Np sorption on the external surface of poorly crystallized ferric oxide. Experiments were performed in a glove box (<1 ppm O_2) filled with highly pure nitrogen (purity=99.999%) at 25°C . The concentrations of Np and Fe were 1×10^{-8} and 1×10^{-2} M, respectively.

that NpO_2^+ has a high affinity for PCFO. There was no measurable shift in the Np sorption curve with a change in ionic strength, suggesting that NpO_2^+ is sorbed on the external sites of PCFO by formation of an inner-sphere complex [18]. The formation of a NpO_2^+ inner-sphere complex has been also observed in the NpO_2^+ -quartz system [19].

Table 1 shows the Np distribution between the bulk aqueous phase and the external surface of PCFO. We illustrate the adsorption isotherms of 1 and 96 h in Fig. 3. For the elapsed time from 1 to 96 h, no change in the sorbed amount of Np was observed. Dzombak and Morel [20] showed that the required time to reach sorption equilibrium increased with the ratio of Cd concentration to Fe concentration and a pseudo-equilibrium was reached in 4 h when Cd and total Fe concentrations were 5.5×10^{-7} M and 5×10^{-3} M, respectively. In our experimental system, the sorption of Np on the external surface of PCFO rapidly reaches pseudo-equilibrium within 1 h and the amount of intraparticle diffusion seems to be insignificant. From Fig. 3, we could evaluate the sorption ratio, K_d (ml g^{-1}), of Np at 2.2×10^3 (ml g^{-1}). Fig. 3 also shows a linear relationship between Np sorbed and Np present in the bulk aqueous phase.

3.2. Sorption in micropores

Fig. 4 illustrates the fraction of Np sorbed on PCFO as a function of elapsed time at pH=6. The vertical axis represents the ratio (%) of Np sorbed at each elapsed time to Np sorbed at elapsed time=1920 h. It was found that the Np concentration in the liquid phase did not change after 1920 h.

Considering the experimental and analytical studies of Axe and Anderson [9,10], these results strongly suggest that NpO_2^+ is also sorbed on PCFO by the two-step sorption process. The first step is the rapid sorption onto the external surface and macropore sites, and the second step is the slow sorption onto the internal surface and micropore sites. The latter step is the rate-limiting reaction. Considering the diffusion and the mass balance of Np in a spherical PCFO particle and assuming the linear isotherm and the insignificant pore diffusion [21], the concentration of Np sorbed, C_s , can be written as follows [9],

$$\frac{C_s}{C_0} = 1 + \frac{2R}{\pi r} \sum \frac{(-1)^n}{n} \sin \frac{n\pi r}{R} \exp\left(\frac{-Dn^2\pi^2 t}{R^2}\right), \quad (1)$$

where $D = D_s / (1 + \varepsilon / \rho K C_1)$, R is the radius of sphere and C_0 the concentration of Np sorbed on the external surface, ε the porosity (0.5), D_s the surface diffusion coefficient, and r the radial position in the sphere. We assumed that the density ρ (1.75 g cm^{-3}) of PCFO was same as that used by Axe and Anderson [9]. K is the equilibrium constant of the sorption reaction, $\text{NpO}_2^+ + \langle \text{Fe} \rangle \rightleftharpoons \langle \text{Fe} \rangle - \text{NpO}_2^+$

Table 1

Np concentration in liquid and solid phases in isotherm experiments.

1 h								
Initial Np concentration [M]	1.0×10^{-9}	5.0×10^{-9}	1.0×10^{-8}	3.0×10^{-8}	5.0×10^{-8}	7.0×10^{-8}	1.0×10^{-7}	
Np concentration in liquid phase [M]	2.5×10^{-10}	1.2×10^{-9}	2.5×10^{-9}	7.5×10^{-9}	1.3×10^{-8}	1.8×10^{-8}	2.5×10^{-8}	
Np sorbed on solid phase [mol g ⁻¹ -solid phase]	4.7×10^{-10}	2.4×10^{-9}	4.8×10^{-9}	1.4×10^{-8}	2.3×10^{-8}	3.3×10^{-8}	4.7×10^{-8}	
2 h								
Initial Np concentration [M]	1.0×10^{-9}	5.0×10^{-9}	1.0×10^{-8}	3.0×10^{-8}	5.0×10^{-8}	7.0×10^{-8}	1.0×10^{-7}	
Np concentration in liquid phase [M]	2.5×10^{-10}	1.2×10^{-9}	2.5×10^{-9}	7.3×10^{-9}	1.3×10^{-8}	1.8×10^{-8}	2.6×10^{-8}	
Np sorbed on solid phase [mol g ⁻¹ -solid phase]	4.7×10^{-10}	2.4×10^{-9}	4.7×10^{-9}	1.4×10^{-8}	2.3×10^{-8}	3.3×10^{-8}	4.6×10^{-8}	
4 h								
Initial Np concentration [M]	1.0×10^{-9}	5.0×10^{-9}	1.0×10^{-8}	3.0×10^{-8}	5.0×10^{-8}	7.0×10^{-8}	1.0×10^{-7}	
Np concentration in liquid phase [M]	2.6×10^{-10}	1.2×10^{-9}	2.6×10^{-9}	7.5×10^{-9}	1.3×10^{-8}	1.7×10^{-8}	2.5×10^{-8}	
Np sorbed on solid phase [mol g ⁻¹ -solid phase]	4.7×10^{-10}	2.4×10^{-9}	4.7×10^{-9}	1.4×10^{-8}	2.3×10^{-8}	3.3×10^{-8}	4.7×10^{-8}	
24 h								
Initial Np concentration [M]	1.0×10^{-9}	5.0×10^{-9}	1.0×10^{-8}	3.0×10^{-8}	5.0×10^{-8}	7.0×10^{-8}	1.0×10^{-7}	
Np concentration in liquid phase [M]	2.5×10^{-10}	1.2×10^{-9}	2.7×10^{-9}	7.6×10^{-9}	1.2×10^{-8}	1.8×10^{-8}	2.5×10^{-8}	
Np sorbed on solid phase [mol g ⁻¹ -solid phase]	4.7×10^{-10}	2.4×10^{-9}	4.6×10^{-9}	1.4×10^{-8}	2.6×10^{-8}	3.1×10^{-8}	4.7×10^{-8}	
48 h								
Initial Np concentration [M]	1.0×10^{-9}	5.0×10^{-9}	1.0×10^{-8}	3.0×10^{-8}	5.0×10^{-8}	7.0×10^{-8}	1.0×10^{-7}	
Np concentration in liquid phase [M]	2.4×10^{-10}	1.2×10^{-9}	2.6×10^{-9}	7.4×10^{-9}	1.3×10^{-8}	1.7×10^{-8}	2.6×10^{-8}	
Np sorbed on solid phase [mol g ⁻¹ -solid phase]	4.7×10^{-10}	2.4×10^{-9}	4.6×10^{-9}	1.6×10^{-8}	2.3×10^{-8}	3.3×10^{-8}	4.6×10^{-8}	
96 h								
Initial Np concentration [M]	1.0×10^{-9}	5.0×10^{-9}	1.0×10^{-8}	3.0×10^{-8}	5.0×10^{-8}	7.0×10^{-8}	1.0×10^{-7}	
Np concentration in liquid phase [M]	2.5×10^{-10}	1.2×10^{-9}	2.5×10^{-9}	7.4×10^{-9}	1.3×10^{-8}	1.7×10^{-8}	2.5×10^{-8}	
Np sorbed on solid phase [mol g ⁻¹ -solid phase]	4.7×10^{-10}	2.4×10^{-9}	4.7×10^{-9}	1.5×10^{-8}	2.3×10^{-8}	3.3×10^{-8}	4.7×10^{-8}	

where $\langle \text{Fe} \rangle$ is the available site on and in the PCFO particle. C_t is the total number of sites in PCFO and approximately equal to the available sites, namely the concentration of $\langle \text{Fe} \rangle$. Therefore, KC_t was equal to the ratio of the concentration of Np sorbed to the Np concentration in liquid phase, which could be calculated from Fig. 4. In the present work, KC_t was multiplied by the fraction of sites located internally (0.25). Integrating Eq. (1) over the volume of a sphere gives the amount (M_s) of Np sorbed on a particle at specific times [9],

The amount of Np sorbed on the internal surface was estimated by summing up the M_s times the number of

particles of a given radius for all particles over the entire particle size distribution (Fig. 1). Total amount of Np sorbed on PCFO was calculated from this amount plus the amount of Np sorbed on the external surface, and fitted to the experimental result by a fitting parameter of D_s . A best fitting result is also shown in Fig. 4. The value of optimized D_s of NpO_2^+ was $2.0 \times 10^{-13} \text{ cm}^2 \text{ s}^{-1}$. The calculated result agreed relatively well with the experimental result. This successful fitting also suggests that the sorption of NpO_2^+ on PCFO includes the two-step process and that the pore diffusion of Np was not significant in our

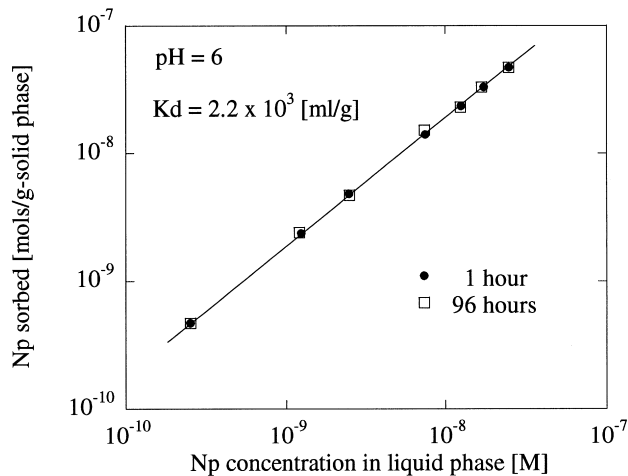


Fig. 3. Isotherm of Np sorption on the external surface of poorly crystallized ferric oxide at pH=6. Experimental data at 1 h and 96 h are illustrated. Other data are shown in Table 1. K_d (ml g⁻¹) is sorption ratio.

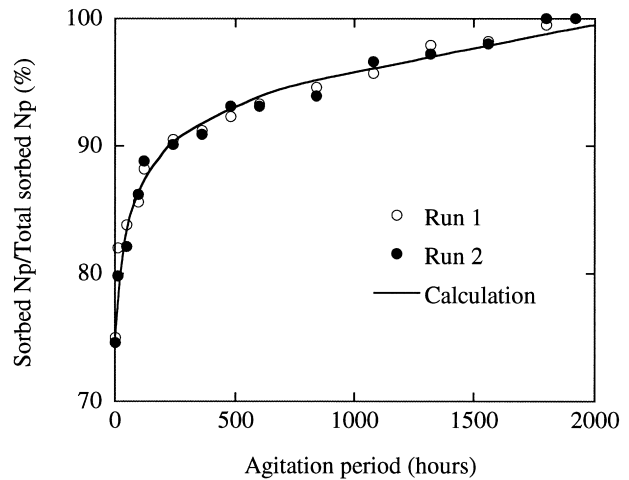


Fig. 4. Fractionation of Np sorbed on poorly crystallized ferric oxide by a constant boundary condition technique at pH=6. Solid line represents the calculated amount of Np sorbed. Vertical axis represents the ratio (%) of Np sorbed at each time to Np sorbed at 1920 h.

study. In this calculation, we used the particle size distribution of Fig. 1. However, we must be aware of the possibility that larger particles mask the presence of smaller particles. In the near future, we will check the particle size distribution and re-evaluate D_s more precisely if necessary.

Furthermore, according to Fig. 2, it seems that the diffusive processes to micropores do not start in four days. However, we can hardly consider that such processes begin suddenly after four days. In the present work, we show that NpO_2^+ sorption to PCFO includes a two-step process, but can not show when the second step starts. We recognize that we have to discuss and elucidate the sorption mechanism in detail in future work.

4. Conclusions

It was strongly suggested that NpO_2^+ is sorbed on PCFO by a two-step sorption process. The first step is the rapid sorption onto the external surface and macropore sites by formation of an inner-sphere complex, and the second step is the slow sorption onto the internal surface and micropore sites. The sorption of Np on the external surface of PCFO rapidly reaches pseudo-equilibrium within 1 h. A linear relationship between Np sorbed on the external surface and Np present in the bulk aqueous phase was observed. Sorption ratio, Kd (ml g^{-1}), was evaluated at $Kd=2.2 \times 10^5 \text{ ml g}^{-1}$. By using a constant boundary condition technique, the rate-limiting process, intraparticle diffusion, was studied. Approximately 25% of the sorption sites are considered to be located on the internal surface and the sorption equilibrium of NpO_2^+ on the internal surface sites was reached in about 1920 h. By taking account of these two steps and the mass balance of NpO_2^+ in PCFO, the diffusion model was applied to the experimental results. The calculated result agreed relatively

well with the experimental result and the surface diffusion coefficient of NpO_2^+ was evaluated at $2.0 \times 10^{-13} \text{ cm}^2 \text{ s}^{-1}$.

References

- [1] J.I. Kim in: A.J. Freeman, C. Keller, (Eds.), Handbook on the Physics and Chemistry of Actinides, Vol. 4, North Holland, Amsterdam, 1986, Chap. 8.
- [2] J. Ahn, T. Ikeda, T. Ohe, T. Kanno, Y. Sakamoto, T. Chiba, M. Tsukamoto, S. Nakayama, S. Nagasaki, K. Banno, T. Fujita, J. At. Energy Soc. Japan, 37 (1995) 59 (in Japanese).
- [3] E.A. Jenne, Symposium on Molybdenum in the Environment, Dekker, 1977.
- [4] D.C. Girvin, L.L. Ames, A.P. Schwab, J.E. McGarrah, J. Colloid Interface Sci. 141 (1991) 67.
- [5] J.S. Herman, Eng. Geol. 26 (1989) 301.
- [6] R.J. Serne, R.C. Arthur, K.M. Krupka, NUREG/CR-558, Pacific Northwest Laboratory, 1990.
- [7] A.N. Sharpley, Soil Sci. Soc. Am. J. 51 (1987) 912.
- [8] M. Sayin, A.R. Mermut, H. Tiessen, Soil Sci. Soc. Am. J. 54 (1990) 1298.
- [9] L. Axe, P.R. Anderson, J. Colloid Interface Sci. 175 (1995) 157.
- [10] L. Axe, P.R. Anderson, J. Colloid Interface Sci. 185 (1997) 436.
- [11] G.W. Bruemmer, J. Gerth, K.J. Tiller, J. Soil Sci. 39 (1988) 37.
- [12] C.C. Fuller, J.A. Davis, G.A. Waychunas, Geochim. Cosmochim. Acta 57 (1993) 2271.
- [13] G.A. Waychunas, B.A. Rea, C.C. Fuller, J.A. Davis, Geochim. Cosmochim. Acta 57 (1993) 2251.
- [14] D.S. Wisnubroto, S. Nagasaki, Y. Enokida, A. Suzuki, Solvent Extr. Ion Exch. 11 (1993) 377.
- [15] E. Matijevic, P. Scheiner, J. Colloid Interface Sci. 63 (1978) 509.
- [16] H. Nitsche, Radiochim. Acta 52–53 (1991) 3.
- [17] V. Neck, J.I. Kim, B. Kanellakopulos, Radiochim. Acta 56 (1992) 25.
- [18] K.F. Hayes, Ph.D. thesis, Stanford University, Stanford, 1987.
- [19] S. Tanaka, S. Nagasaki, H. Itagaki, M. Yamawaki, Proc. 1989 Joint Inter. Waste Management Conf., vol. II, 1989, p. 375.
- [20] D.A. Dzombak, F.M.M. Morel, J. Colloid Interface Sci. 112 (1986) 588.
- [21] G.F. Froment, K.B. Bischoff, Chemical Reactor Analysis and Design, Wiley, New York, 1990.